

PROCESS MODELLING OF ANIONICALLY POLYMERISED POLYAMIDE-6 FOR APPLICATION IN THERMOPLASTIC REACTIVE RESIN TRANSFER MOULDING (R-RTM)

Jarrad Humphry¹, Nan Yang¹, Luigi-Jules Vandi², Rowan Truss¹, Darren J. Martin³ and Michael T. Heitzmann¹

¹School of Mechanical and Mining Engineering, The University of Queensland, St Lucia, Australia
Email: jarrad.humphry@uqconnect.edu.au

Email: n.yang@uq.edu.au

Email: r.truss@uq.edu.au, Web Page: <http://www.chemeng.uq.edu.au/truss>

Email: m.heizmann@uq.edu.au, Web Page: <http://researchers.uq.edu.au/researcher/10496>

²School of Chemical Engineering, The University of Queensland, St Lucia, Australia

Email: l.vandi@uq.edu.au, Web Page: <http://researchers.uq.edu.au/researcher/2503>

³Australian Institute for Bioengineering and Nanotechnology (AIBN), The University of Queensland,
St Lucia, Australia

Email: d.martin@uq.edu.au, Web Page: <http://researchers.uq.edu.au/researcher/650>

Keywords: reactive processing, anionic polymerisation, polyamide-6, thermoplastic composites

Abstract

The reactive processing of thermoplastics holds great promise for the rapid manufacture of tough composites for semi-structural applications, especially in the automotive sector. Anionically Polymerised Polyamide-6 (APA6) is a leading candidate for reactive processing among thermoplastics which forms the focus of this work. However, the reactive pathway for the in situ formation of thermoplastic composites is yet to be exploited commercially. A significant roadblock to their use is a lack of system understanding and poor reproducibility in terms of properties and degree of conversion. In this, in situ processing of thermoplastics is a particular complication from the traditional manufacture of thermosets or melt processing of thermoplastics due to interplay of the variables: conversion, crystallinity, and viscosity. As processing is ideally conducted below the final melting temperature of the matrix (to both significantly reduce the time to solidification and the thermal degradation of the matrix), the ring opening polymerisation of the monomer, and the crystallisation of these newly formed polymer chains occurs simultaneously. The degree and effect of this interplay defines the final monomer conversion and polymer crystallinity and ultimately the mechanical properties of the composite. This work presents modelling activities undertaken through the following of the thermal process of the reaction by Differential Scanning Calorimetry (DSC), fitting kinetic and crystallisation models, and developing a so-called Time-Temperature Transformation (TTT) diagram to aid in process design and parameter selection. An example TTT diagram is shown in Fig. 1. These models are then compared to thermal profile and properties of a composite part manufactured through Reactive-Resin Transfer Moulding (R-RTM) of the APA6 system. This work presents a methodology for the generation of these TTT diagrams as well as highlights further complications in regards to the modelling of the system, most significantly its sensitivity to oxygen, moisture, and catalyst aging.

1. Introduction

Thermoplastic composites are an emerging class of materials which occupy a similar niche to thermosetting composites, along with enhanced machinability, weldability, and superior toughness. Due to the high melt viscosity of thermoplastics, the manufacture of these composites presents unique

challenges. One way of overcoming this challenge of high melt viscosities is through the use of reactive processing, in which the product thermoplastic is polymerised *in situ* (in mould or otherwise), allowing for rapid impregnation of the fibres and mould filling by the low viscosity monomer.

One such reactive thermoplastic system is the anionic ring-opening polymerisation of ϵ -caprolactam to form polyamide-6. This system however gives rise to complex simultaneous behaviours of polymerisation, crystallisation, and, critically for processing considerations, the corresponding viscosity increase and ultimate part solidification. Some research into these systems [1–5] showed a sensitivity of product polymer quality to processing conditions such as temperature, catalyst concentrations and ratios. The development of kinetic polymerisation, crystallisation, and rheological (chemorheological) models is thus critical for the quality assurance of the product thermoplastic parts, as well as the optimisation of the manufacturing processes used to manufacture them (including minimising time to demould, anticipating shrinkage, etc.). Also of interest is the development of Time-Temperature Transformation (TTT) diagrams such as those typically used for thermosetting resins, which may be used as practical processing guidelines. Such diagrams have been developed for the PA12 reactive system [6], and for the PA6 reactive system [7], though different heating regimes, catalysts and catalyst concentrations must be explored independently.

Perhaps the most straightforward way to obtain kinetic data for an exothermic process is through calorimetry, as the rate of each process will be directly proportional to the corresponding heat release. In literature, this has been conducted through the use of a double-walled glass reaction vessel with the corresponding temperature gain measured [8, 9], and through the use of Differential Scanning Calorimetry (DSC), whereby the heat release rate can be more directly measured [10, 11]. As polymerisation and crystallisation may occur simultaneously in these systems, care must be taken to separate the thermal contribution of each before modelling the kinetics [10, 11]. For slow polymerisation processes analysed through DSC, this has been conducted by Taki et al. (2016) [11] through a peak separation algorithm, including the fitting of two asymmetric Gaussian functions whereby the area of the curve associated with crystallisation is set to the area of the subsequent melting (after further heating) of the polymer crystals (see Eq. 1-4).

The generally accepted model for the reaction kinetics of the anionic polymerisation of caprolactam is the Kamal-Sourour model (see 3.3 Model Fitting – Eq. 5 & 6) [8, 11, 14]. This model was originally used for the curing kinetics of thermosetting materials [15]. The model is semi-mechanistic, in that it attempts to model the reaction with a first order reaction term (which is proportional to the remaining unreacted monomer), and an autocatalytic term (which is proportional to the conversion). The model has two Arrhenius reaction rate constants (k_1 , k_2) each with an activation energy (E_A) and Arrhenius constant (A), and two reaction indices (m , n), giving six free parameters in total.

An understanding of the viscosity profile of the reaction system is critical from a processing perspective. Critically, for the infusion of fabrics the time taken to reach a viscosity of ~ 1 Pa.s governs the processing window of the system. Teuwen (2011) [16] provides a review of several viscosity models, relating system viscosity to the degree of conversion and monomer viscosity at the same temperature. The simplest of these models is presented in Eq. 3, this was originally presented for this reactive system by Sibal et al. (1983) [17]. The monomer viscosity may also be modelled through the use of an Arrhenius model such as that presented in Eq. 7 & 8 [4].

2. Materials & Sample Preparation

Brüggemann Chemicals' TM Brüggolen [®] reactive system was used in this study to investigate the anionic polymerisation of polyamide-6. This system uses an initiator, Magnesium Bromide Caprolactamate 'C1', and activator, N,N'-hexane-1,6-diylbis(hexahydro-2-oxo-1H-azepine-1-carboxamide ('C20P'), along with a special dry grade ϵ -caprolactam ('AP-CL'). The monomer (ϵ -

Athens, Greece, 24-28th June 2018

3

caprolactam), undergoes ring-opening to form polyamide-6, initiated and activated by the two catalysts, which allows the reaction to occur below 200 °C, with reaction temperatures as low as 140 °C possible. Catalyst molar concentrations of 1.2 mol% initiator and 0.4 mol% activator (by active ingredient).

All sample preparation, including weighing, melting, and mixing was conducted in an MBraun Dry Nitrogen Glovebox (water and oxygen content was below 10 ppm for the duration of all preparation). In order to achieve a consistent reaction profile, excellent mixing and dispersion is required. This was achieved by:

1. Careful weighing and mixing of ~10g batches of ϵ -caprolactam and catalysts.
2. This mixture was then thoroughly ground using a mortar & pestle until a visually homogenous mixture was obtained.
3. The mixture was gently heated (to 80 °C) on a hot plate and the resulting melt gently stirred.
4. The vessel was allowed to cool and recrystallise.
5. The resulting solid mixture was then sampled by scraping with a spatula. The top surface was discarded to avoid any surface effects (i.e. atmosphere exposure).
6. This powder was then added to Thermal Analysis Tzero hermetically sealed DSC pans and crimped to seal. Each pan contained 5-15 mg of mixture. The pans were visually inspected to ensure they were sealed.

3. Methodology

3.1 Differential Scanning Calorimetry (DSC)

A Q2000 series Thermal Analysis DSC was used with a heating regime consisting of a heating ramp (30 °C/min) to isothermal temperature (40 minute hold) followed by further heating to allow for melting of the polymer (10 °C/min), and finally cooling to ambient temperature (10 °C/min). This test was conducted for three temperatures, at 150 °C, 160 °C, and 170 °C, each in triplicate with average values used. Tzero hermetic sealed pans were used to prevent the evaporation of the monomer during the heating process.

3.2 Extracting Kinetic Data

A procedure similar to that used by Taki et al. [11] was used to convert the exothermic heat flow observed in the isothermal trace to kinetic conversion data.

1. The onset and conclusion of the reaction peak was obtained through analysis of the first derivative of heat flow (y-axis in the DSC traces).
2. A dual asymmetric Gaussian curve fitting was conducted to separate the thermal contribution of the polymerisation from that of the crystallisation. Each Gaussian function is a three parameter model (a_i, b_i , and c_i) as seen in Eq. 2 & 3. The parameters were determined through a non-linear model fitting minimising the error between f (in Eq. 1) and the measured polymerization curve. The equations were additionally constrained by Eq. 4, setting the area under the crystallisation curve to that of that measured in the controlled heating. The area of the second curve was set to the enthalpy of the corresponding melting peak in the second (10 °C/min) heating. The first Gaussian curve (chronologically) now approximates the thermal contribution of polymerisation to the isothermal trace.

$$f = f_p + f_c \quad (1)$$

$$f_p = \begin{cases} a_p \exp\left(-\frac{(t - b_p)^2}{2c_{p1}^2}\right) & (t \leq b_p) \\ a_p \exp\left(-\frac{(t - b_p)^2}{2c_{p2}^2}\right) & (t > b_p) \end{cases} \quad (2)$$

$$f_c = \begin{cases} a_c \exp\left(-\frac{(t - b_c)^2}{2c_{c1}^2}\right) & (t \leq b_c) \\ a_c \exp\left(-\frac{(t - b_c)^2}{2c_{c2}^2}\right) & (t > b_c) \end{cases} \quad (3)$$

$$\Delta H_f = \int_{t_1}^{t_2} f_c dt \quad (4)$$

Where the subscripts ‘p’ and ‘c’ represent polymerisation and crystallisation respectively. a correspond to peak height and b represents peak-onset time. ΔH_f is the measured heat of fusion of PA6 crystals in the subsequent melting following polymerisation. t_1 and t_2 are the times immediately before and after the polymerisation/crystallisation process.

3. This curve may then be converted to conversion (β) by considering the relative cumulative integral. Complete conversion ($\beta = 1$), is considered the final equilibrium state of the polymer and monomer, though some residual monomer may remain (1-3%). This should be considered through separate analysis after the reaction is complete, by Thermogravimetric Analysis (TGA) or solid extraction techniques (e.g. Soxhlet extraction).

3.3 Model Fitting

The extracted conversion data was then used to find parameters for the Kamal-Sourour model (Eq. 5). Where β is the monomer conversion, t is the time, m and n are reaction indicies, and k_1 and k_2 are Arrhenius reaction constants which are each dependent on temperature by Eq. 6. A simple rheokinetic model is included in Eq. 7 & 8 [16]. Where η is the effective viscosity, η_{mon} is the effective viscosity of the monomer, and k is a constant. A value of k in Eq. 7 of 21.6 [-] has been used in this work [16].

$$\frac{\partial \beta}{\partial t} = (k_1 + k_2 \beta^m)(1 - \beta)^n \quad (5)$$

$$k_i = A_i \exp\left(-\frac{E a_i}{RT}\right) \quad (6)$$

$$\eta = \eta_{mon} \times \exp(k\beta) \quad (7)$$

$$\eta_{mon} = 2.7 \times 10^{-7} \text{ Pa.s} \times \exp(3525/T) \quad (8)$$

4. Results & Discussion

Fig. 2 shows the DSC trace showcasing the four heating cycles including the rapid initial heating (1), isothermal hold (2), controlled heating (3), and controlled cooling (4). These heating regimes show monomer melting, polymerisation and crystallisation exotherm (see Fig. 3), polymer melting, and polymer crystallisation respectively. From the controlled heating cycle the enthalpy of melting is recorded (in this case, 48.42 J/g). A polymer melt temperature of 220 °C is typical for polyamide-6.

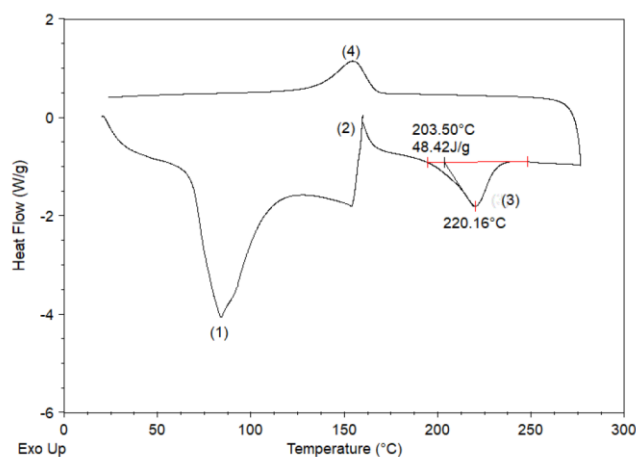


Figure 2. Differential Scanning Calorimetry (DSC) scan of the reactive mixture prepared in Tzero Hermetically Sealed Pans. The reactive mixture consists of C1/C20P at 1.2 mol% and 0.4 mol% respectively with balance ϵ -caprolactam. Four heating regimes include rapid heating (30 °C/min) to isothermal temperature (160 °C), 40 minute isothermal hold, controlled heating (10 °C/min) to 280 °C, and controlled cooling (-10 °C/min) to room temperature. Features of the graph include (1) Monomer melting, (2) Isothermal – reaction exotherm, (3) Polymer melting, and (4) Polymer crystallisation.

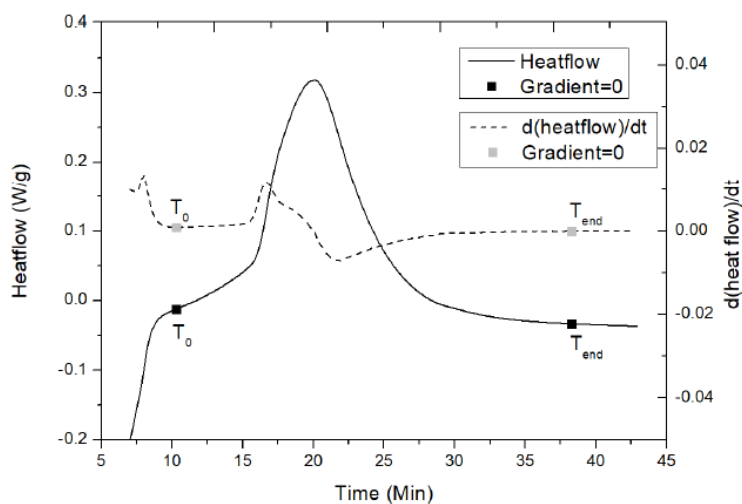


Figure 3. Isothermal heating region of Fig. 2 (2). Heat flow is presented as a solid line, first derivative as a dashed line, squares highlight the points of zero gradient, marking the onset and conclusion of the reaction exotherm.

Fig. 3 shows the isothermal heating cycle corresponding to the (2) in Fig. 2. The onset and conclusion of the polymerisation exotherm has been identified by finding the points surrounding the curve where the first derivative is zero. This reaction exotherm was then separated into a polymerisation and crystallisation through model fitting of Eq. 1-4.

An example separation result is presented in Fig. 4. The effectiveness of the model to separate the polymerisation and crystallisation processes accurately can be inferred by the difference between the true heat flow data and that of the sum of the calculated polymerisation and crystallisation heat flow data (“Calculation” in Fig. 4). This error may be due to additional kinetic effects, including interaction between polymerisation and crystallisation, additional reactions, or secondary crystallisation.

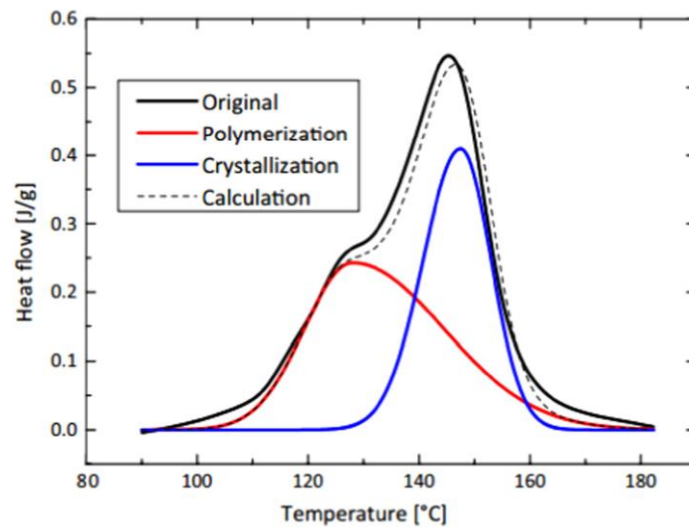


Figure 4. Curve separated isothermal exotherm showing polymerisation (first curve – red) and crystallisation (second curve – blue). The solid line shows the true exotherm value whilst the dotted line shows the sum of the polymerisation and crystallisation curves.

The resulting polymerisation enthalpy curve is directly correlated to the degree of conversion. This data can be used to fit the parameters of the Kamal-Sourour model (Eq. 5 & 6) as outlined in 3.3 Model Fitting. The results for this parameter fitting based on three isothermal datasets (at 150 °C, 160 °C, and 170 °C) are presented in Table 1.

Table 1. Parameter for the Kamal-Sourour Kinetic Model for C1/C20P initiator/activator system with three datasets at 150, 160, and 170 °C

Concentration		Kamal-Sourour model fitting						
Init.	Act.	A_1	A_2	E_{a1}	E_{a2}	m	n	R^2
mol%	mol%	$10^3/s$	$10^5/s$	kJ/mol	kJ/mol	-	-	%
1.2	0.4	2.49	2.920	63.023	60.389	1.107	1.335	95.51

Athens, Greece, 24-28th June 2018

7

The kinetic parameters presented in table 1, along with the crystallisation data (presented in increments of 10%) obtained from the peak separation, and the viscosity model adapted from Teuwen 2011 (Eq. 7) [16], a time-temperature transformation (TTT) diagram was generated (Fig. 5).

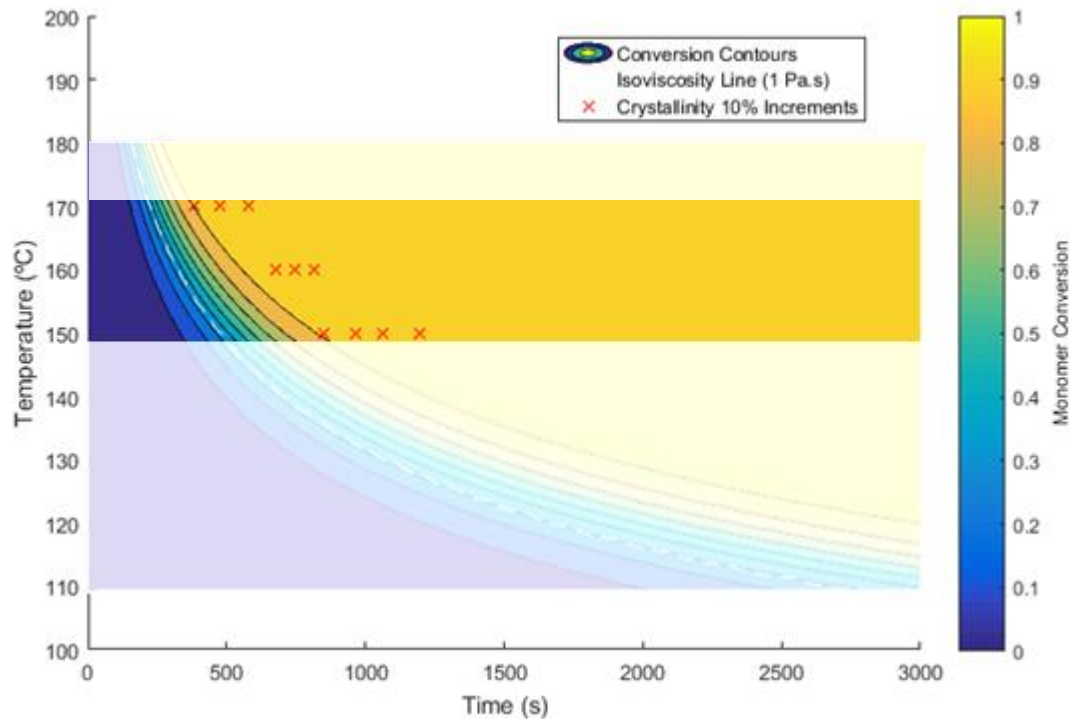


Figure 5. A demonstration of a Time-Temperature Transformation (TTT) diagram, obtained from the peak separation and kinetic analysis of reaction and crystallisation thermal data obtained through Differential Scanning Calorimetry (DSC). The isoviscosity line (dashed) is fit to the conversion based on the Sibal model adapted by Teuwen [16], discussed in text. The resin system is that of the Anionic Polymerisation of ϵ -caprolactam to form polyamide-6 (APA6) with the Brüggemann Chemicals' Brüggolen® catalyst system: C1 & C20P with a molar concentration of 1.2 mol% and 0.4 mol% respectively. The graph presented includes extrapolation indicated by wash-out. The diagram based on isothermal datasets at 150 °C, 160 °C, and 170 °C only.

5. Conclusions, Limitations, & Directions

The resulting time-temperature transformation diagram allows for the (reasonable) extrapolation of conversion and crystallisation. This, in turn, allows for the modelling of injection/infusion processes, and ultimately for the selection of processing conditions to achieve the desired reaction time. It is notable that due to the nature of the differential equation used in this model, that is it strictly only valid for isothermal heating regimes. If the departure from true behaviour is significant it may be necessary to generate TTT diagrams based on more reasonable reaction thermal profiles, i.e. with a constant heating rate or under a (quasi-)adiabatic conditions. Additionally, the testing conditions here necessitate the use of a premixed initiator and activator, whereas in practical application the activator and initiator would only be mixed upon injection. This means in practical application, the reaction rate may differ depending on the method of combination. Furthermore, different catalyst systems and concentrations, along with a wider range of temperatures and heating regimes are required to generate a more complete picture of the processing window of this reactive system. Additionally, further work is required in the modelling of the crystallisation kinetics.

Acknowledgments

The authors wish to thank the Australian National Fabrication Facility ANNF-Q for the use of their inert atmosphere dry nitrogen MBraun Glovebox critical to the experimental work in this study.

References

- [1] K. Udipi, R. Dave, R. Kruse, and L. Stebbins, "Polyamides from lactams via anionic ring-opening polymerization: 1. Chemistry and some recent findings," *Polymer (Guildf.)*, vol. 38, no. 4, pp. 927–938, 1997.
- [2] R. S. Dave, R. L. Kruse, K. Udip, and D. E. Williams, "Polyamides from Lactams via anionic ring- opening polymerization: 3. Rheology," *Polymer (Guildf.)*, vol. 38, no. 4, pp. 949–954, 1997.
- [3] R. S. Dave, R. L. Kruse, L. R. Stebbins, and K. Udipi, "Polyamides from lactams via anionic ring-opening polymerization: 2. Kinetics," *Polymer (Guildf.)*, vol. 38, no. 4, pp. 939–947, 1997.
- [4] J. J. E. Teuwen, A. van Geenen, and H. E. N. Bersee, "Vacuum-infused anionic polyamide-6 composites: The effect of postprocessing," *J. Thermoplast. Compos. Mater.*, vol. 25, no. 8, pp. 965–986, 2011.
- [5] K. van Rijswijk and H. E. N. Bersee, "Reactive processing of textile fiber-reinforced thermoplastic composites - An overview," *Compos. Part A Appl. Sci. Manuf.*, vol. 38, no. 3, pp. 666–681, 2007.
- [6] A. Luisier, P.-E. Bourban, and J.-A. E. Manson, "Time–Temperature–Transformation Diagram for Reactive Processing of Polyamide 12," *J. Appl. Polym. Sci.*, vol. 81, pp. 963–972, 2001.
- [7] A. Maazouz, K. Lamnawar, and M. Dkier, "Chemorheological study and in-situ monitoring of PA6 anionic-ring polymerization for RTM processing control," *Compos. Part A Appl. Sci. Manuf.*, 2018.
- [8] J. J. E. Teuwen, A. A. Van Geenen, and H. E. N. Bersee, "Novel reaction kinetic model for anionic polyamide-6," *Macromol. Mater. Eng.*, vol. 298, no. 2, pp. 163–173, 2013.
- [9] A. Y. Malkin, S. L. Ivanova, V. G. Frolov, A. N. Ivanova, and Z. S. Andrianova, "Kinetics of Anionic Polymerization of Lactam. (Solution of Non-isothermal kinetic problems by the inverse method)," vol. 20, pp. 1791–1800, 1980.
- [10] N. Barhoumi, A. Maazouz, M. Jaziri, and R. Abdelhedi, "Polyamide from lactams by reactive rotational molding via anionic ring-opening polymerization: Optimization of processing parameters," *Express Polym. Lett.*, vol. 7, no. 1, pp. 76–87, 2013.
- [11] K. Taki, N. Shoji, M. Kobayashi, and H. Ito, "A kinetic model of viscosity development for in situ ring-opening anionic polymerization of ϵ -caprolactam," *Microsyst. Technol.*, 2016.
- [12] T. Ageyeva, I. Sibikin, and J. Karger-Kocsis, "Polymers and related composites via anionic ring-opening polymerization of lactams: Recent developments and future trends," *Polymers*. 2018.
- [13] J. Humphry, L. Jules-Vandi, R. Truss, D. J. Martin, and M. T. Heitzmann, "Process Modelling in Anionically Polymerised Polyamide-6 (APA6) for the in situ polymerisation of Composite Matrices," in *Special Issue 1st International Symposium on Advanced Composites*, 2017.
- [14] S. Russo, S. Maniscalco, and L. Ricco, "Some new perspectives of anionic polyamide 6 (APA 6) synthesis," *Polym. Adv. Technol.*, vol. 26, no. 7, pp. 851–854, 2015.
- [15] M. R. Kamal and S. Sourour, "Kinetics and thermal characterization of thermoset cure," *Polym. Eng. Sci.*, vol. 13, no. 1, pp. 59–64, 1973.
- [16] J. J. E. Teuwen, "Thermoplastic Composite Wind Turbine Blades," 2011.